Functional optoacoustic neuro-tomography of calcium fluxes in adult zebrafish brain in vivo

Deán-Ben, X Luís ; Gottschalk, Sven ; Sela, Gali ; Shoham, Shy ; Razansky, Daniel

DOI: https://doi.org/10.1364/ol.42.000959

Functional optoacoustic neuro-tomography of calcium fluxes in adult zebrafish brain *in-vivo*

X. Luís Deán-Ben,[1] Sven Gottschalk,[1] Gali Sela,[1] Shy Shoham,[2] Daniel Razansky[1,3,*]

[1]*Institute for Biological and Medical Imaging (IBMI), Helmholtz Center Munich, Neuherberg, Germany*
[2]*Department of Biomedical Engineering, Technion – Israel Institute of Technology, Haifa, Israel*
[3]*School of Medicine, Technical University of Munich, Germany*
**Corresponding author: dr@tum.de*

Received 11 November 2016; revised 14 January 2017; accepted 6 February 2017; posted 6 February 2017 (Doc. ID 280563); published 27 February 2017

Genetically encoded calcium indicators (GECIs) have revolutionized neuroimaging by enabling mapping the activity of entire neuronal populations *in vivo*. Visualization of these powerful activity sensors has so far been limited to depth-restricted microscopic studies due to intense light scattering in the brain. We demonstrate, for the first time, *in vivo* real-time volumetric optoacoustic monitoring of calcium transients in adult transgenic zebrafish expressing the GCaMP5G calcium indicator. Fast changes in optoacoustic traces associated with GCaMP5G activity were detectable in the presence of other strongly absorbing endogenous chromophores, such as hemoglobin. The new functional optoacoustic neuroimaging method can visualize neural activity at penetration depths and spatio-temporal resolution scales not covered with the existing neuroimaging techniques.

OCIS codes: *(110.5120) Photoacoustic imaging, (000.1430) Biology and medicine, (170.3880) Medical and biological imaging*

https://doi.org/10.1364/OL.42.000959

Brains of complex organisms process information using sequences of action potentials at scales ranging from local microcircuits of neighboring neurons to complex neural networks of more than ten billion cells [1, 2]. Identifying the complex spatio-temporal activity patterns in different areas of the brain is thus essential for a better understanding of the principles of neuronal signal processing [3]. In this regard, imaging of genetically encoded calcium indicators (GECI) arguably represents one of the most versatile approaches for investigating brain function [4-6] that can simultaneously detect activity from a significantly higher number of neurons as compared to the conventional electrode-based electrophysiological recordings [2]. To this end, GECIs have been widely employed for probing neuronal activity on a large range of spatio-temporal scales [7, 8].

More efficient probes are continuously being engineered [7-10]. Of particular relevance is the family of GCaMP proteins, which modulate fluorescent intensity as a function of intracellular calcium concentration [11, 12]. As opposed to small-molecule-based calcium indicators, GECIs can be specifically expressed in specific types of cells [9]. In addition, new GCaMPs have been shown to outperform synthetic calcium indicators in sensitivity and speed, in a way that it was possible to detect, under certain conditions, fluorescent signals from single action potentials in intact brains [13]. Despite remarkable progress on the development of neuronal activity labels, the inherent penetration limitations of optical microscopy currently impose the most significant barrier for large-scale monitoring of brain activity. For instance, typical imaging depth of up to 0.5-1 mm and effective field-of-view well below $1mm^3$ of the most advanced two photon microscopy systems [14] make whole-brain in-vivo imaging only possible for simple or transparent organisms. An additional limitation lies in the effective spatio-temporal resolution range of state-of-the-art scanning-based microscopes, i.e. the number of voxels that can be effectively acquired in real time [15].

Optoacoustic imaging can overcome the light diffusion limitations by ultrasonically resolving light absorption distribution at depths of several millimeters to centimeters in biological tissues [16] and was previously shown capable of whole-brain imaging in mice at near-infrared wavelengths [17]. Optoacoustic tomographic image acquisition is based on simultaneous excitation of an entire imaged volume with a single laser pulse. Thus, the effective volumetric imaging rate is solely determined by the pulsed repetition frequency of the laser [18]. Therefore, real-time 3D imaging at wide range of spatio-temporal scales can be enabled [19]. Optoacoustics has also shown good sensitivity in detecting GCaMP5G signals induced by neural activity *ex vivo* in isolated brain preparations and in living transparent larvae [19]. As opposed to the majority of fluorescent calcium indicators, which mainly operate by changing their quantum yield as a function of calcium concentration, the GCaMP5G as well as most other indicators from the GCaMP family exhibit strong variations in the

absorption cross-section in response to neural activity, a desirable feature for optoacoustic neuroimaging.

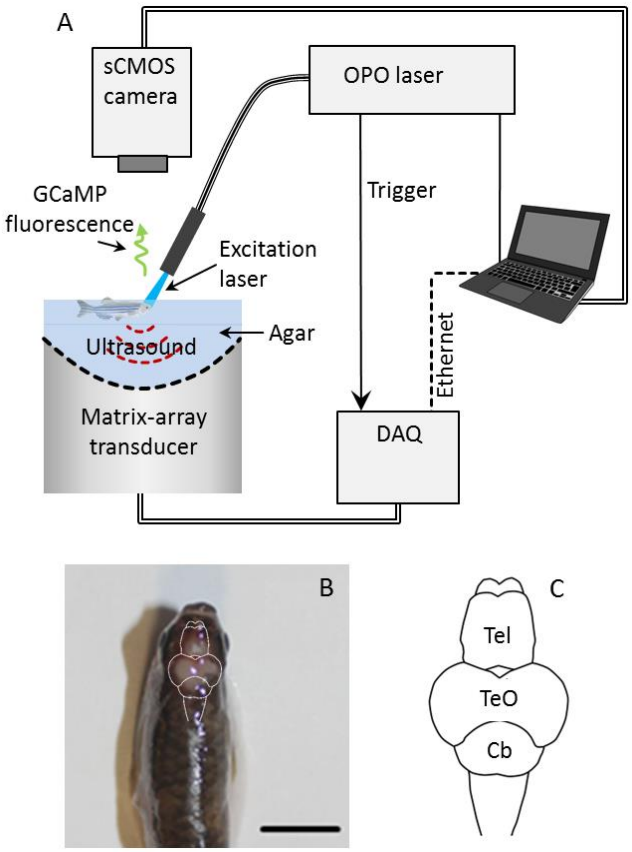

Fig. 1. (A) Layout of the experimental system. DAQ – data acquisition system. (B) Actual photograph of the zebrafish taken after the imaging experiment. Scalebar – 4mm. (C) Schematic drawing indicating the main functional areas in adult zebrafish brain (also superimposed in panel B. Tel – telencephalon, TeO – optic tectum, Cb – cerebellum.

Herein, we investigate the feasibility of imaging calcium transients in the whole brain of a live adult zebrafish expressing the genetically encoded GCaMP5G indicator in a large fraction of its neurons. This represents a challenging environment for imaging as endogenous chromophores in the fish generate strong optoacoustic signals that may conceal responses from the calcium indicators. A lay-out of the experimental system employed is depicted in Fig. 1A. A previously reported spherical matrix array detector was used to collect three-dimensional optoacoustic images of the fish. The array consists of 256 densely-distributed piezocomposite detection elements with 4 MHz central frequency and a -6 dB bandwidth of 100% [20]. The individual elements have an approximate size of 3x3mm^2. The spherical array has a surface with 40 mm radius of curvature and angular coverage of 90°. Its active surface was covered with agar gel to guarantee acoustic coupling to the imaged specimen. A nearly isotropic resolution in the range of 200 μm is attained in the focal area of the spherical array geometry [20]. An adult (1.5 months old) wildtype HuC:GCAMP5G zebrafish was anesthetized with 0.015% of Tricaine solution and its skull was gently removed. The animal was then placed inside a groove made in the agar gel. Optoacoustic excitation was provided with an optical parametric oscillator (OPO)-based laser tuned to a wavelength of 488 nm (close to the peak excitation frequency of calcium-saturated GCaMP5G) and operated at pulse repetition frequency of 25 Hz with <5% pulse-to-pulse energy fluctuations. To further minimize the effects of laser instability, the acquired optoacoustic signals were normalized using a photodiode readings. The light beam was guided with a custom-made fiber bundle to illuminate the brain, as illustrated in Fig. 1A. Optoacoustic reconstructions were performed using an iterative model-based algorithm described in detail in [21]. The fluorescence induced responses were simultaneously acquired with a high speed sCMOS camera (Model: pco.edge 4.2, PCO AG, Kelheim, Germany) containing a longpass filter for isolating the GCaMP5G fluorescence. The integration time of the camera was set to 200 ms. Handling, anesthesia, and imaging of zebrafish were all performed in full compliance with the institutional guidelines of the Helmholtz Center Munich and with approval from the Government District of Upper Bavaria under animal protocol reference number 55.2-1-54-2532-57-2016. Animals were euthanized by overdose of Tricane immediately after the imaging session.

An actual photograph of the fish taken ex-vivo after the imaging experiment is displayed in Fig. 1B. Brain vasculature and other pigmentation, which produce strong background optoacoustic responses at the 488 nm peak excitation wavelength of the GCaMP5G probe, are clearly visible.

To elicit calcium transients, 50 mM Pentylenetetrazole (PTZ) was applied via a syringe pump (flow rate of ~5 μL/s, volume 100-200 μL) in the vicinity of the brain surface. PTZ is a blocker of the gamma amino butyric acid (GABA) receptor channel and is widely utilized to induce seizures in the zebrafish model [22]. The epifluorescence images for four different instants post injection of PTZ are displayed in Fig. 2A while the corresponding maximum intensity projections (MIPs) of the simultaneously acquired three dimensional optoacoustic images are shown in Fig. 2B. The entire acquired temporal image sequences are further available in Visualization 1. To better distinguish the GCaMP-related activity, Figs. 2C,D show temporal evolution of the differential optoacoustic signal $\Delta OA=OA-OA_0$ in individual slices lying at different depths in the brain. The baseline signal OA_0 for each pixel was taken as an average of 10 optoacoustic signal values preceding the PTZ-induced activation. Furthermore, a median filter over a window of 5 frames was applied to the optoacoustic signal traces. This additional filtering step is necessary to reduce noise in the signal traces while better preserving the high frequency information in comparison with a simple smoothing (low pass) filter. Even though the epi-fluorescence recordings represent planar (surface-projected) contributions of the GCaMP signal, we attempted to directly compare between planar epifluorescence and volumetric optoacoustic recordings by selecting approximately matching regions of interest (ROIs) indicated by circles in Figs. 2A-D, whose temporal traces are presented in Figs. 2E and 2F. Note that one ROI representing a background region outside the brain (purple circle) was also analyzed but the relative optoacoustic signal variations have been only manifested inside the brain. The relative variations of the fluorescence signals in the approximately corresponding ROIs are displayed in Fig. 2G.

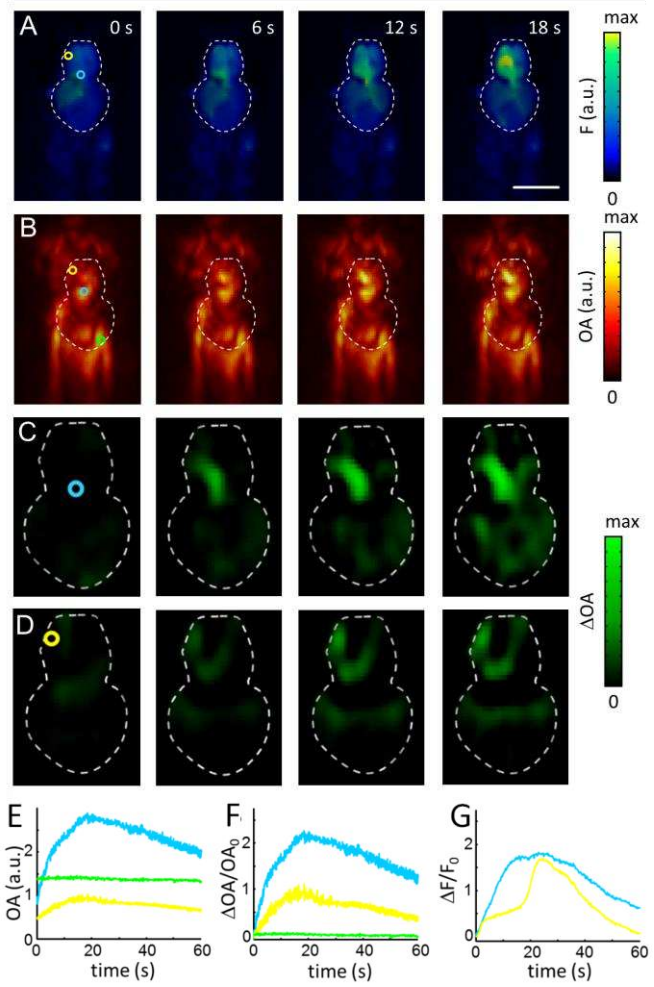

Fig. 2. Imaging of neuronal activation in adult zebrafish brain following application of pentylenetetrazole. (PTZ) (A) Time course of planar epi-fluorescence images following injection of the agent at t = 0 s. (B) The corresponding MIPs along the depth direction of the three-dimensional optoacoustic images; (C), (D) Temporal evolution of the differential optoacoustic signal $\Delta OA=OA-OA_0$ in individual slices lying at average depths of 400 μm and 1.3 mm beneath the brain surface, respectively. Scalebar – 3 mm. (E) Optoacoustic time traces from the ROIs marked by circles in panels b-d; (F) Corresponding time traces of the fractional optoacoustic signal variations $\Delta OA/OA_0$; (G) Fractional fluorescence signal variations for the ROIs marked by circles in panel a. The entire image sequence can be visualized in a supplementary video file (Visualization 1).

While similar levels of relative signal increase due to calcium activity are observed in both fluorescence ($\Delta F/F_0$) and optoacoustic ($\Delta OA/OA_0$) modes, the overall signal variations turn to be different, which can be best appreciated in Visualization 1. This is generally expected because the planar epi-fluorescence images merely represent averaged (surface-projected) measurements lacking resolution in the depth direction, whereas optoacoustic measurements provide true volumetric traces. Furthermore, optoacoustic images exhibit much stronger tissue background (Fig. 2B, 0 s), which arises from strong absorption by intrinsic tissue chromphores, presumably hemoglobin and melanin. Nevertheless, the maximum optoacoustic signal changes generated by activated GCaMP5G is comparable in its magnitude to the signal associated to background tissue components (Fig. 2B, 18 s).

The presented results demonstrate, for the first time, the basic feasibility of optoacoustic monitoring of neural activity in a living adult zebrafish brain expressing genetically-encoded calcium indicators. In particular, strong calcium transients were optoacoustically detected in the presence of significant tissue background due to strong absorption by intrinsic tissue chromophores at 488 nm, peak absorption wavelength of the GCaMP5G protein. Several key limitations ought to be addressed before functional optoacoustic neuroimaging can be broadly applied for calcium imaging deep in scattering brains. While our method has demonstrated sufficient sensitivity for detecting strong calcium fluxes due to direct injection of neurostimulant into the brain, its detection sensitivity for other (physiologically relevant) stimuli must be established. Also, our current proof of concept experiments were done using a low resolution imaging setup optimized for imaging large tissue volumes, whereas cellular resolution is essential for accurate recording and interpretation of large-scale neural activity. In order to achieve such resolution performance, the ultrasonic detection bandwidth of the matrix array elements should be increased beyond 40 MHz, a challenging objective for the piezoelectric detection technology. Propagation of high frequency optoacoustic field is also significantly hampered by acoustic attenuation and strong speed of sound mismatches introduced by the skull [23, 24]. Note that, since a wild type adult zebrafish was used in our current experiments, skin and skull covering the brain area were removed in order to avoid light reflection and strong absorption by the skin pigmentation. Finally, when considering imaging larger brains, such as a whole mouse brain, the labeling approaches should be optimized for near-infrared excitation wavelengths enabling deeper light penetration [16]. While optical microscopy suffers from limited imaging depth due to scattering and has further limitations in terms of attainable spatio-temporal resolution and field of view, the optoacoustic technology is ideally suited for simultaneous large-scale recording of entire volumes containing millions of neurons. Thus, future far-red and near-infrared GECIs providing high fractional changes in their absorbance in response to calcium fluctuations may then serve to visualize never-seen-before large-scale neuronal activity patterns in mammals.

In conclusion, we have demonstrated, for the first time to our knowledge, that optoacoustic imaging allows mapping calcium transients *in vivo* in an adult vertebrate organism with highly absorbing endogenous background. State-of the-art volumetric optical microscopy has significantly better spatial resolution dictated by the optical diffraction limit, but its typical fields of view are also orders of magnitude smaller, rendering those methods incapable of large-scale recordings from entire scattering brains. Conversely, macroscopic methods, such as fMRI or optical diffusion techniques, can visualize whole brain volumes but their spatio-temporal performance is inferior to real-time volumetric optoacoustic imaging and their signal is mainly limited to slow and indirect hemodynamic changes due to neuronal activity. Finally, since it was previously demonstrated that optoacoustics is ideally tailored for probing the hemodynamic parameters of the brain in action [25], the newly discovered capacity for simultaneous imaging of calcium indicators can be potentially exploited to

facilitate investigations into the mechanisms of neurovascular coupling. Thus, functional optoacoustics can provide unprecedented neuroimaging capabilities at penetration scales and spatio-temporal resolution levels not covered with existing imaging modalities.

Funding. German-Israeli Foundation for ScientificResearch and Development (GIF) (1142-46.10/2011); European Research Council (ERC) (ERC-2015-CoG-682379); National Institutes of Health (NIH) (R21 EY026382-01).

Acknowledgment. The authors thank A. Lauri and G. G. Westmeyer for kindly providing the specimen and for helpful discussions.

REFERENCES

1. F. Helmchen and M. Hubener, "Neuronal networks in the spotlight: deciphering cellular activity patterns with fluorescent proteins," Neuroforum **19**, 47-55 (2013).
2. S. Kim and S. B. Jun, "In-vivo optical measurement of neural activity in the brain," Experimental neurobiology **22**, 158-166 (2013).
3. S. Peron, T.-W. Chen, and K. Svoboda, "Comprehensive imaging of cortical networks," Current opinion in neurobiology **32**, 115-123 (2015).
4. L. L. Looger and O. Griesbeck, "Genetically encoded neural activity indicators," Current Opinion in Neurobiology **22**, 18-23 (2012).
5. H. Mutoh and T. Knopfel, "Probing neuronal activities with genetically encoded optical indicators: from a historical to a forward-looking perspective," Pflug Arch Eur J Phy **465**, 361-371 (2013).
6. G. J. Broussard, R. Q. Liang, and L. Tian, "Monitoring activity in neural circuits with genetically encoded indicators," Front Mol Neurosci **7**(2014).
7. J. Akerboom, N. C. Calderon, L. Tian, S. Wabnig, M. Prigge, J. Tolo, A. Gordus, M. B. Orger, K. E. Severi, J. J. Macklin, R. Patel, S. R. Pulver, T. J. Wardill, E. Fischer, C. Schuler, T. W. Chen, K. S. Sarkisyan, J. S. Marvin, C. I. Bargmann, D. S. Kim, S. Kugler, L. Lagnado, P. Hegemann, A. Gottschalk, E. R. Schreiter, and L. L. Looger, "Genetically encoded calcium indicators for multi-color neural activity imaging and combination with optogenetics," Front Mol Neurosci **6**(2013).
8. S. Tang, F. Reddish, Y. Zhuo, and J. J. Yang, "Fast kinetics of calcium signaling and sensor design," Curr Opin Chem Biol **27**, 90-97 (2015).
9. M. Inoue, A. Takeuchi, S. Horigane, M. Ohkura, K. Gengyo-Ando, H. Fujii, S. Kamijo, S. Takemoto-Kimura, M. Kano, J. Nakai, K. Kitamura, and H. Bito, "Rational design of a high-affinity, fast, red calcium indicator R-CaMP2," Nature methods **12**, 64-70 (2015).
10. L. Tian, S. A. Hires, T. Mao, D. Huber, M. E. Chiappe, S. H. Chalasani, L. Petreanu, J. Akerboom, S. A. McKinney, E. R. Schreiter, C. I. Bargmann, V. Jayaraman, K. Svoboda, and L. L. Looger, "Imaging neural activity in worms, flies and mice with improved GCaMP calcium indicators," Nature methods **6**, 875-U113 (2009).
11. J. Akerboom, T. W. Chen, T. J. Wardill, L. Tian, J. S. Marvin, S. Mutlu, N. C. Calderon, F. Esposti, B. G. Borghuis, X. R. Sun, A. Gordus, M. B. Orger, R. Portugues, F. Engert, J. J. Macklin, A. Filosa, A. Aggarwal, R. A. Kerr, R. Takagi, S. Kracun, E. Shigetomi, B. S. Khakh, H. Baier, L. Lagnado, S. S. H. Wang, C. I. Bargmann, B. E. Kimmel, V. Jayaraman, K. Svoboda, D. S. Kim, E. R. Schreiter, and L. L. Looger, "Optimization of a GCaMP Calcium Indicator for Neural Activity Imaging," J Neurosci **32**, 13819-13840 (2012).
12. T. Knopfel, "Genetically encoded optical indicators for the analysis of neuronal circuits," Nat Rev Neurosci **13**, 687-700 (2012).
13. T. W. Chen, T. J. Wardill, Y. Sun, S. R. Pulver, S. L. Renninger, A. Baohan, E. R. Schreiter, R. A. Kerr, M. B. Orger, V. Jayaraman, L. L. Looger, K. Svoboda, and D. S. Kim, "Ultrasensitive fluorescent proteins for imaging neuronal activity," Nature **499**, 295-+ (2013).
14. J. N. D. Kerr and W. Denk, "Imaging in vivo: watching the brain in action," Nat Rev Neurosci **9**, 195-205 (2008).
15. E. E. Hoover and J. A. Squier, "Advances in multiphoton microscopy technology," Nat Photonics **7**, 93-101 (2013).
16. X. L. Deán-Ben, T. F. Fehm, M. Gostic, and D. Razansky, "Volumetric hand-held optoacoustic angiography as a tool for real-time screening of dense breast," Journal of biophotonics (2015).
17. S. Gottschalk, T. F. Fehm, X. L. Dean-Ben, and D. Razansky, "Noninvasive real-time visualization of multiple cerebral hemodynamic parameters in whole mouse brains using five-dimensional optoacoustic tomography," J Cerebr Blood F Met **35**, 531-535 (2015).
18. X. L. Dean-Ben, S. J. Ford, and D. Razansky, "High-frame rate four dimensional optoacoustic tomography enables visualization of cardiovascular dynamics and mouse heart perfusion (vol 5, 10133, 2015)," Sci Rep-Uk **5**(2015).
19. X. L. Deán-Ben, G. Sela, A. Lauri, M. Kneipp, V. Ntziachristos, G. G. Westmeyer, S. Shoham, and D. Razansky, "Functional optoacoustic neuro-tomography (FONT) for scalable whole-brain monitoring of calcium indicators," Light Sci Appl **5**, e16201 (2016).
20. X. L. Dean-Ben and D. Razansky, "Portable spherical array probe for volumetric real-time optoacoustic imaging at centimeter-scale depths," Optics express **21**, 28062-28071 (2013).
21. X. L. Dean-Ben, A. Buehler, V. Ntziachristos, and D. Razansky, "Accurate Model-Based Reconstruction Algorithm for Three-Dimensional Optoacoustic Tomography," IEEE transactions on medical imaging **31**, 1922-1928 (2012).
22. K. Wong et al. "Modeling seizure-related behavioral and endocrine phenotypes in adult zebrafish", Brain Res **1348**, 209-215 (2010).
23. X. L. Dean-Ben, D. Razansky, and V. Ntziachristos, "The effects of acoustic attenuation in optoacoustic signals," Physics in medicine and biology **56**, 6129-6148 (2011).
24. H. Estrada, J. Rebling, J. Turner, and D. Razansky, "Broadband acoustic properties of a murine skull," Physics in medicine and biology **61**, 1932 (2016).
25. J. J. Yao, L. D. Wang, J. M. Yang, K. I. Maslov, T. T. W. Wong, L. Li, C. H. Huang, J. Zou, and L. V. Wang, "High-speed label-free functional photoacoustic microscopy of mouse brain in action," Nature methods **12**, 407-+ (2015).